Interleukin-4 promotes microglial polarization toward a neuroprotective phenotype after retinal ischemia/reperfusion injury

https://doi.org/10.4103/1673-5374.339500

Date of submission: April 23, 2021

Date of decision: June 16, 2021

Date of acceptance: February 22, 2022

Date of web publication: April 29, 2022

Di Chen[1, 2, #], Cheng Peng[1, 2, #], Xu-Ming Ding[1, 2], Yue Wu[1, 2], Chang-Juan Zeng[1, 2], Li Xu[1, 2, *], Wen-Yi Guo[1, 2, *]

From the Contents

Introduction	2755
Materials and Methods	2756
Results	2758
Discussion	2759

Graphical Abstract *IL-4 administration prolongs the duration of M2 microglia polarization and reduces the loss of retinal ganglion cells after retinal ischemia/reperfusion surgery*

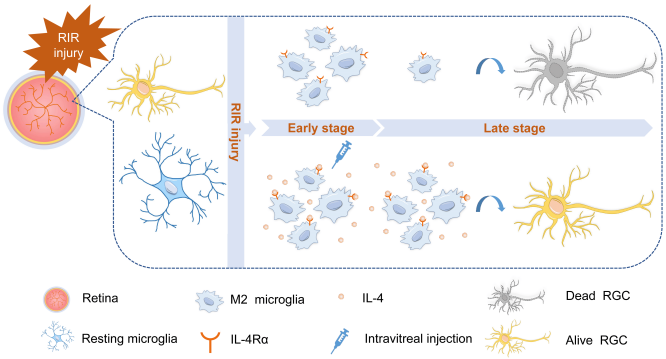

Abstract

Glaucoma results from irreversible loss of retinal ganglion cells (RGCs) through an unclear mechanism. Microglial polarization and neuroinflammation play an important role in retinal degeneration. Our study aimed to explore the function of microglial polarization during glaucoma progression and identify a strategy to alleviate retinal neuroinflammation. Retinal ischemia/reperfusion injury was induced in C57BL/6 mice. In a separate cohort of animals, interleukin (IL)-4 (50 ng/mL, 2 μL per injection) or vehicle was intravitreally injected after retinal ischemia/reperfusion injury. RGC loss was assessed by counting cells that were positive for the RGC marker RNA binding protein, mRNA processing factor in retinal flat mounts. The expression of classically activated (M1) and alternatively activated (M2) microglial markers were assessed by quantitative reverse transcription-polymerase chain reaction, immunofluorescence, and western blotting. The results showed that progressive RGC loss was accompanied by a continuous decrease in M2 microglia during the late phase of the 28-day period after retinal ischemia/reperfusion injury. IL-4 was undetectable in the retina at all time points, and intravitreal IL-4 administration markedly improved M2 microglial marker expression and ameliorated RGC loss in the late phase post-retinal ischemia/reperfusion injury. In summary, we observed that IL-4 treatment maintained a high number of M2 microglia after RIR and promoted RGC survival.

Key Words: glaucoma; hyper-intraocular pressure; *in vivo*; interleukin-4; intravitreal injection; M2 microglia; neurodegeneration; neuroprotective effect; retinal ganglion cell; retinal ischemia-reperfusion

Introduction

Glaucoma is a group of heterogeneous diseases characterized by progressive degeneration of retinal ganglion cells (RGCs) and clinical visual field defects and is a leading cause of irreversible blindness worldwide (Tham et al., 2014). Safe and effective therapies for this disease are lacking (Quigley, 2011). While the factors that contribute to the loss of RGCs have not been fully elucidated, inflammation within the retina is strongly associated with optic nerve damage and neurodegeneration (Williams et al., 2017). Importantly, microglia play a crucial role in neuroinflammation, which is a key process in glaucoma (Grassivaro et al., 2020; Zhang et al., 2021). Microglial activation has been reported in specimens from patients with glaucoma and in animal models of glaucoma (Agarwal and Agarwal, 2017).

Microglia are resident innate immune cells in neural tissue, act as neuropathological sensors, and represent the first line of defense against injury in the central nervous system (CNS), including in the brain and retina (Streit et al., 2005). After trauma occurs, microglia respond by undergoing morphological and functional changes and producing cytokines, which further promote neuroinflammation. Activated microglia can switch between two polarized phenotypes (Burma et al., 2017; Lan et al., 2017). "Classically activated" M1 microglia are characterized by the production of proinflammatory cytokines, such as interleukin (IL)-1β, tumor necrosis factor-α, and IL-6, and increased expression of inducible nitric oxide synthase (iNOS) and the surface markers CD86, CD16/32, and CD40; these molecules are indispensable for pathogen clearance but also induce damage in normal adjacent tissue, which contributes to neuronal loss and neurotoxicity (Kalkman and Feuerbach 2016). "Alternatively activated" M2 microglia release anti-inflammatory cytokines and growth factors and express specific markers, such as CD206, arginase 1 (ARG1), IL-10, transforming growth factor-β, chitinase-like 3 (YM1 in rodents, Chl3L3 in humans), and the resistin protein FIZZ1 (Kronenberg et al., 2018; Song et al., 2019; Zheng et al., 2019; Kobashi et al., 2020; Chen et al., 2021). CD206 and ARG1 are typical markers used to identify M2 microglia (Miron et al., 2013; Zanier et al., 2014). These two paradoxical states are associated with different microenvironmental signals. In particular, under *in vitro* conditions, lipopolysaccharide and interferon-γ stimulate M1 polarization of microglia (Hu et al., 2012; Miron et al., 2013). In contrast, anti-

[1]Department of Ophthalmology, Ninth People's Hospital, Shanghai Jiao Tong University School of Medicine, Shanghai, China; [2]Shanghai Key Laboratory of Orbital Diseases and Ocular Oncology, Shanghai, China

*Correspondence to: Li Xu, PhD, x_jenny_dr@hotmail.com; Wen-Yi Guo, PhD, wyguo9h@163.com.

https://orcid.org/0000-0002-9379-1301 (Li Xu); https://orcid.org/0000-0002-0723-6353 (Di Chen)

#Both authors contributed equally to this work.

Funding: *This work was supported by the National Natural Science Foundation of China, No. 81970796 (to WYG), Clinical Research Program of the Ninth People's Hospital, Shanghai Jiao Tong University School of Medicine, No. JYLJ201905 (to WYG), Interdisciplinary Program of Shanghai Jiao Tong University, No. YG2019QNA18 (to YW).*

How to cite this article: *Chen D, Peng C, Ding XM, Wu Y, Zeng CJ, Xu L, Guo WY (2022) Interleukin-4 promotes microglial polarization toward a neuroprotective phenotype after retinal ischemia/reperfusion injury. Neural Regen Res 17(12):2755-2760.*

inflammatory M2 polarization (Olah et al., 2012; Miron et al., 2013) is induced by the anti-inflammatory cytokines IL-4, IL-10, and IL-13.

IL-4 is a multifunctional cytokine that is primarily secreted by Th2 lymphocytes and regulates a variety of immune-related activities. IL-4 binds to the IL-4 receptor α (IL-4Rα) chain, which is followed by the recruitment of a γ-chain or IL-13 receptor α1 to form IL-4 type I or II complexes, respectively (LaPorte et al., 2008). Subsequently, these complexes initiate tyrosine phosphorylation of STAT6 and activate the classical STAT6 signaling cascades to support M2 activation (Murray et al., 2014; Han et al., 2015; Xiong et al., 2015).

The polarization pattern of retinal microglia during RGC loss after retinal ischemia/reperfusion (RIR) injury remains unclear. Moreover, little is known regarding how IL-4 affects microglial polarization and RGC survival in the retina, the elucidation of which may contribute to future therapies for glaucoma or other neurodegenerative diseases. As a common subtype of glaucoma, acute angle-closure glaucoma is an emerging medical condition that occurs when intraocular pressure (IOP) is abruptly increased because of obstruction of drainage pathways. RIR is considered a major pathological factor in acute angle-closure glaucoma, and experimentally induced RIR injury is used to investigate the pathogenesis of this type of glaucoma (Mathew et al., 2019). The aim of the present study was to explore the role of microglial polarization in the pathogenesis of RGC loss after RIR injury and discover methods to improve RGC survival by altering the bias or duration of microglial polarization.

Materials and Methods

Animals

Approximately 200 specific pathogen-free, female C57BL/6 mice were used in this study. Mice were 8–10 weeks old and weighed 19–23 g. All mice were purchased from Shanghai Slac Laboratory Animal Co, Ltd (Slac, Shanghai, China; license No. SCXK (Hu) 2017-0005) and were raised in the animal facility under specific pathogen-free conditions with a 12-hour light/dark cycle and access to water and normal diet food *ad libitum*. All animal experiments were approved by the Medical Animal Care & Welfare Committee of the Ninth People's Hospital, Shanghai Jiao Tong University School of Medicine on December 26, 2018 (approval No. HKDL [2018]495) and conducted in accordance with the standards of the Association for Research in Vision and Ophthalmology. This study was reported in accordance with the ARRIVE 2.0 guidelines (Animal Research: Reporting of *In Vivo* Experiments; Percie du Sert et al., 2020).

Experiment I

RIR model

An RIR model was established as previously described (Hartsock et al., 2016). Briefly, mice were anesthetized by intraperitoneal injection of 1% pentobarbital sodium (50 mg/kg; Merck, Kenilworth, NJ, USA, Cat# P-010-1ML). Procaine eyedrops (4 mg/mL; Santen Pharmaceutical, Shanghai, China) and tropicamide eyedrops (5 mg/mL; Santen Pharmaceutical) were dropped onto the left eye of each mouse for local anesthesia and pupil dilation, respectively. Thereafter, we cannulated the anterior chamber with a 30-gauge needle connected to a 1.2-meter tall saline bottle for 1 hour as shown in **Figure 1A** and **Additional Figure 1**. Only one eye (left side) per mouse was subjected to cannulation. At this time, the IOP was approximately 80 mmHg. The mice were kept on a 37 °C heating pad after the procedure to maintain body temperature until they completely recovered. Mice were sacrificed on days 0, 1, 3, 7, 14, and 28 after RIR surgery. Quantification of CD206$^+$ areas (n = 4–5 mice/group) and quantitative reverse transcription-polymerase chain reaction (qRT-PCR) assays (n = 3–4 mice/group) were performed for RIR mice in the day 0, 3, 7, 14, and 28 groups. Normal control mice, which did not undergo RIR surgery, were sacrificed on corresponding days 3, 7, 14, and 28 days and analyzed as above. The total number of mice used for all experiments was approximately 200 (**Figures 2** and **3**).

Retinal flat mount preparation and immunofluorescent staining

On days 0, 1, 3, 7, 14, and 28 after RIR injury, mice were anesthetized and perfused with 50 mL phosphate-buffered saline (PBS) (Cat# C20012500BT, Gibco, Shanghai, China) to clear blood cells from the vessels followed by 25 mL 4% paraformaldehyde (Sangon Biotech, Shanghai, China, Cat# E672002-0500) for tissue fixation. The eyes were enucleated and fixed in 2% paraformaldehyde for > 24 hours at room temperature. Retinal tissue was obtained by scissoring the eyeballs along the corneoscleral limbus and removing the anterior segment, choroid, and scleral tissues. The retina was then fixed in 2% paraformaldehyde for 30 minutes and washed three times in PBS containing 0.05% Tween 80 (Cat# P1754, MilliporeSigma, Burlington, MA, USA). The retinal tissues were incubated with primary antibodies overnight at 4°C after blocking with 5% donkey serum for 2 hours at room temperature. The following primary antibodies were used: rabbit anti-ionized calcium binding adaptor molecule 1 (IBA1; marker for retinal microglia; 1:1000, Cat# 019-19741, Wako Pure Chemical Industries, Osaka, Japan), goat anti-CD206 (marker for M2 microglia; 1:800, Cat# AF2535, R&D Systems, Minneapolis, MN, USA), rabbit anti-RNA binding protein, mRNA processing factor (RBPMS; marker for RGCs; 1:200, Cat# NBP2-20112, Novus Biologicals, Manchester, UK), and goat anti-ARG1 (1:100, Cat# ab60176, Abcam, Cambridge, UK). The retinas were washed with PBS containing 0.1% Triton X-100 (Cat# T8787, MilliporeSigma) and 0.05% Tween and then incubated with the corresponding secondary antibodies for 2 hours at room temperature as follows: Alexa Fluor 488-conjugated donkey anti-goat antibody (1:500, Cat# A-11055, Thermo Fisher Scientific, Waltham, MA, USA) was used for CD206 and ARG1 staining,

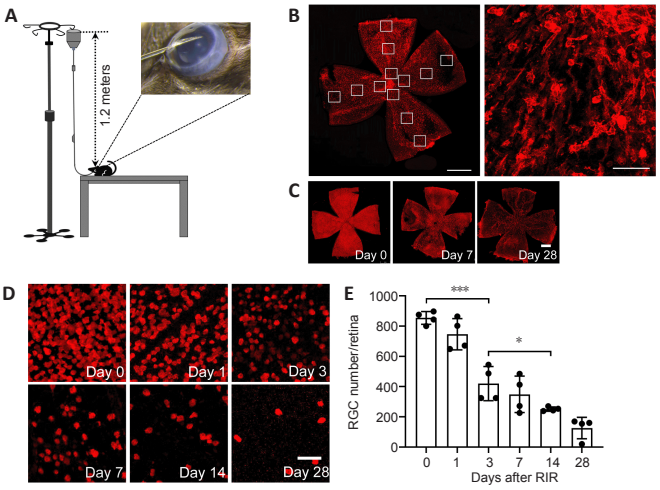

Figure 1 | **RGCs are lost continuously over a 28-day period after RIR injury.**
(A) Schematic diagram of the strategy used to induce RIR injury. A 30-gauge needle connected to 1.2-meter tall saline container was cannulated in the anterior chamber of the mouse eye. (B) Illustration of the strategy used for counting cells in retinal flat mounts. The image on the left shows a whole retinal flat mount photographed at 100× magnification (red: IBA1 [ionized calcium binding adaptor molecule 1], scale bar: 1 mm), and the image on the right shows a part of the flat mount photographed at 200× magnification (scale bar: 50 μm) for cell counting. Each retina was divided into four quadrants with 3 different regions each (highlighted by 12 small white boxes in the retina), i.e., the central, intermediate, and peripheral regions, and the images were captured for cell counting as shown in the right panel. The average cell numbers in these 12 regions were used to calculate the cell density for the entire retina. Changes in RGC numbers on days 0, 1, 3, 7, 14, and 28 after RIR injury are shown in (C) and (D). RNA binding protein, mRNA processing factor (RBPMS; (red) was used as a marker for RGCs. (C) Representative images for the assessment of RBPMS expression within the whole retina (scale bar: 50 μm) showed that RGC loss occurred in a homogeneous fashion over the entire retina, including the region close to the optic nerve head and in the periphery, and the loss became gradually more severe over time. (D) Representative images for RBPMS$^+$ cell counting (scale bar: 1 mm). The RBPMS$^+$ cell numbers decreased and the RBPMS$^-$ regions expanded gradually until almost the entire retina was RBPMS$^-$ by day 28 after RIR surgery. (E) The quantification of RBPMS$^+$ cells in panel D, which represents the average RGC number in retinas from mice at 0, 1, 3, 7, 14, and 28 days after RIR. The bar chart indicated that RGCs were lost continuously within the 28-day period following RIR. Among adjacent time points, the largest RGC reduction occurred between days 1 and 3. On days 7 and 28, the number of RGCs decreased to approximately 50% and 25% of that observed on day 0, respectively. n = 4 mice per group. Data are expressed as the means ± SD; *P < 0.05, ***P < 0.001 (unpaired Student's t-tests). Three independent replicates were measured in each experiment. RGC: Retinal ganglion cell; RIR: retinal ischemia/reperfusion.

Alexa Fluor 594-conjugated donkey anti-rabbit antibody (1:500, Cat# A-21207, Thermo Fisher Scientific) was used for RBPMS staining, and Alexa Fluor 647-conjugated donkey anti-rabbit (1:500, Cat# A-31573, Thermo Fisher Scientific) was used to stain IBA1. Finally, the retinas were washed, flattened on slides, and mounted using antifade mounting medium with DAPI (Cat# P36966, Thermo Fisher Scientific). The slides were stored at 4°C prior to imaging.

Retinal cell densities were measured in 12 areas of each retina: 4 areas in the central retina, 4 areas in the intermediate regions, and 4 areas in the peripheral retina (**Figure 1B**). Cell counting was performed routinely in a blinded manner. Fluorescent images were captured using a confocal laser scanning microscope (LEICA TCS SP5; Leica; Wetzlar, Germany) at 100× and 200× magnification. NIH ImageJ software (v.1.8.0; National Institutes of Health; Bethesda, MD, USA; Schneider et al., 2012) was used to quantify all histological parameters. The quantification was performed as follows. The "8-bit color" tool was used first to convert fluorescent images to grayscale images, and, then, the "threshold" tool was chosen to set the boundaries of positive and negative gray values. For microglial cells, the "area fraction" measurement tool was selected to quantify the percentage of the positive gray value that represented the percentages of ARG1$^+$, CD206$^+$, and IBA1$^+$ areas within the image; for ganglion cells, the particle size was set using the "analysis particles" tool, and the particle counts represented the RBPMS$^+$ cell numbers in the images. For each retina, 12 images distributed over 12 locations were captured as highlighted in the white boxes in **Figure 1B**. The average number of RBPMS+ cells in the 12 images was defined as RGC number/retina. Similarly, the average percentages of ARG1$^+$, CD206$^+$, and IBA1$^+$ areas for the 12 images were defined as the ARG1$^+$ area %, CD206$^+$ area %, and IBA1$^+$ area %.

Retinal protein extraction and western blot analysis

On days 0, 1, 3, 7, 14, and 28 after RIR injury, the mice were anesthetized and perfused with 50 mL PBS through the heart to remove the majority of blood cells from the retinal blood vessels. The retinas were separated from the eyeballs and sonicated in ice-cold RIPA lysis buffer (Cat# 89901, Thermo

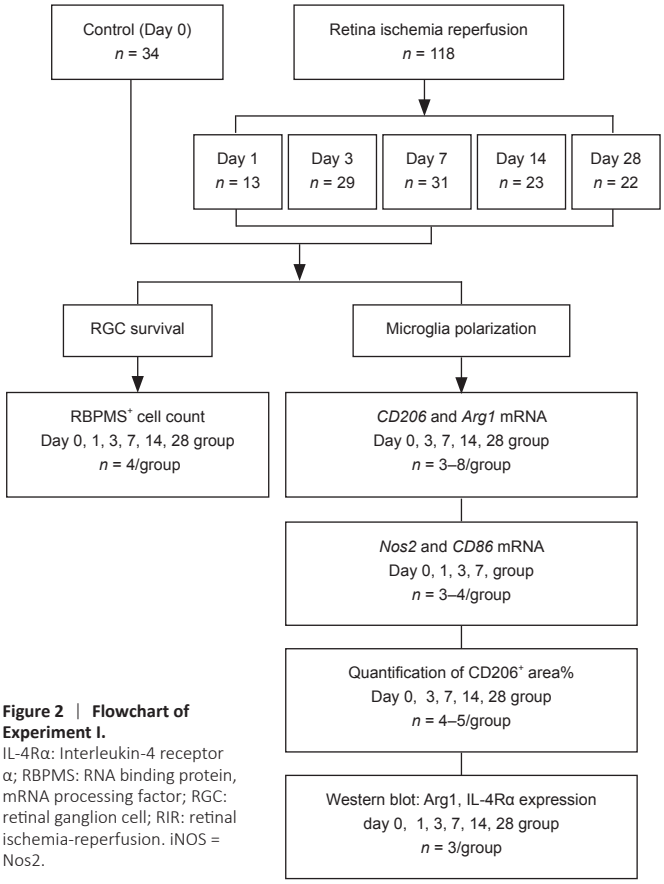

Figure 2 | **Flowchart of Experiment I.**
IL-4Rα: Interleukin-4 receptor α; RBPMS: RNA binding protein, mRNA processing factor; RGC: retinal ganglion cell; RIR: retinal ischemia-reperfusion. iNOS = Nos2.

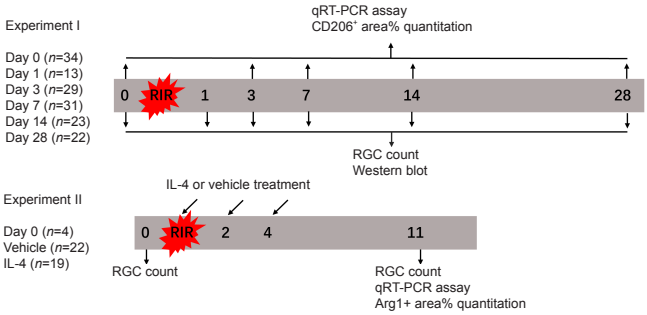

Figure 3 | **Experimental timeline.**
IL: Interleukin; qRT-PCR: quantitative reverse transcription-polymerase chain reaction; RGC: retinal ganglion cell. Nos2=iNOS.

Fisher Scientific) containing a protease inhibitor cocktail (Cat# 4693116001, Merck). The lysate was centrifuged at 12,000 × *g* for 10 minutes at 4°C. The supernatant was collected, and the protein concentration was quantified with a BCA protein assay kit (Cat# 23225, Thermo Fisher Scientific). Protein from each sample was resolved on SDS-PAGE gels and transferred to 0.2 μm polyvinylidene fluoride membranes (Cat# 03010040001, MilliporeSigma). The membranes were blocked with 5% bovine serum albumin (Cat# A602440-0050, Sangon Biotech, Shanghai, China) for 1 hour at room temperature and incubated with primary antibodies overnight at 4°C followed by incubation with fluorophore-conjugated anti-mouse secondary antibodies for 1 hour at room temperature. The primary antibodies used included mouse anti-ARG1 (1:100, Cat# sc-271430, Santa Cruz Biotechnology, Santa Cruz, CA, USA) and mouse anti-β-actin (1:5000, Cat# A5441, MilliporeSigma). Because of the importance of IL-4 in regulating a functional M2 microglial phenotype *in vitro* (Boche et al., 2013; Mantovani et al., 2013), we also used mouse anti-IL-4Rα (1:100, Cat# sc28361, Santa Cruz Biotechnology) and rat anti-IL-4 (1:1000, Cat# MAB404, R&D Systems). The secondary antibodies were DyLight 800-conjugated donkey anti-mouse (1:10,000, Cat# SA5-10172, Thermo Fisher Scientific) and DyLight 755-conjugated donkey anti-mouse (1:10,000, Cat# SA5-10043, Thermo Fisher Scientific) antibodies. Western blot images were captured with the Odyssey Clx Imaging System (Licor Biosciences, Lincoln, NE, USA) and quantitatively analyzed using Image Studio Ver 5.2 software (Licor Biosciences).

Experiment II

IL-4 administration

To determine the potential role of IL-4 and IL-4Rα in RIR injury, we performed intravitreal injections of recombinant IL-4 or vehicle in mice. Initially, we administered a single injection of recombinant IL-4 immediately after RIR injury; however, a single injection failed to affect microglial polarization. Subsequently, we administered three injections of recombinant IL-4 to maintain a relatively high level of IL-4 in the eyes that were subjected to RIR (**Figure 3**). Drug administration was performed on the day of RIR and on days 2 and 4 after RIR. On the day of drug administration, a 33-gauge Hamilton syringe (Hamilton; Reno, NV, USA, Cat# 21-2062) was used for intravitreal injection of mouse recombinant IL-4 (2.0 μL, 50 ng/mL) (Peprotech; Wuhan, China, Cat# 214-14) or PBS into the left eye of each mouse. On day 7 after the last injection, the mice were sacrificed for further analysis. RGC survival evaluation (n = 4–5 mice/group) was performed among the following three groups: (1) normal group: mice that did not go through RIR surgery and drug administration; (2) vehicle group: RIR mice that were treated with vehicle; and (3) IL-4 group: RIR mice that were treated with IL-4. The percentage of ARG1$^+$ areas (n = 4 mice/group) and M2-related gene expression (n = 3–5 mice/group) were compared between the vehicle and IL-4 groups (**Figure 4**). The methods of RIR model establishment, retinal flat mount preparation, RGC and microglia quantitation, retinal RNA preparation, and qRT-PCR were identical to those described above.

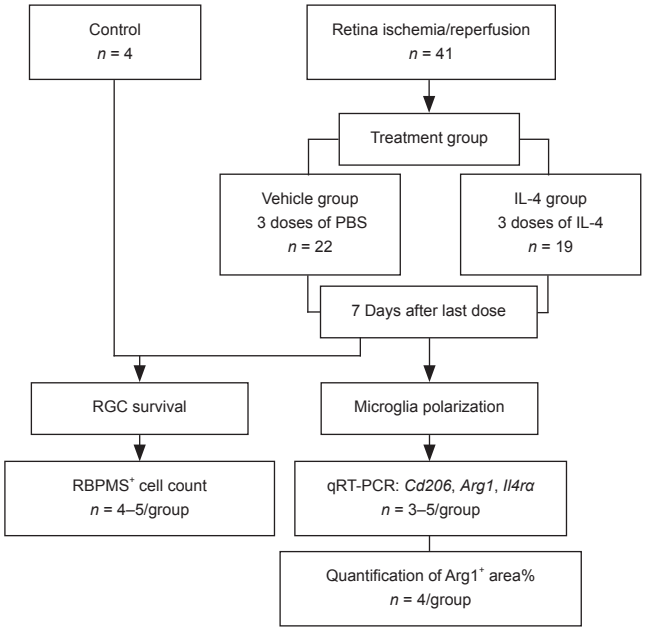

Figure 4 | **Flowchart of Experiment II.**
IL: Interleukin; PBS: phosphate-buffered saline; qRT-PCR: quantitative reverse transcription-polymerase chain reaction; RBPMS: RNA binding protein, mRNA processing factor; RGC: retinal ganglion cell.

Retinal RNA preparation and quantitative reverse transcription-polymerase chain reaction

Mice were anesthetized and perfused transcardially with 50 mL PBS on days 0, 3, 7, 14, and 28 after RIR injury (Experiment I) and 7 days after the last injection of vehicle or IL-4 (Experiment II). The eyeballs were enucleated and placed in a 10-cm dish filled with PBS. After surgical separation of the anterior segment, the retinal tissue was removed from the eyecup by mechanical dissociation of the choroidal and scleral layers. Total retinal RNA was extracted with an RNA Purification Kit (Cat #B0004D, EZbioscience, Shanghai, China) in accordance with the manufacturer's instructions. Complementary DNA was synthesized using a PrimeScript RT Reagent Kit (Cat# RR037A, Takara, Shiga, Japan). The qRT-PCR was performed using the ABI Prism 6000 Sequence Detection System (Applied Biosystems, Waltham, MA, USA) in a volume of 10 μL with PowerUp SYBR Green Master Mix (Cat# 4368708, Thermo Fisher Scientific) following the manufacturers' instructions. The mRNA expression levels were normalized to the levels of the endogenous reference gene β-actin. Relative mRNA levels were calculated using the comparative $2^{-\Delta\Delta ct}$ method. The qRT-PCR conditions were as follows: denaturation at 95°C for 5 minutes followed by 40 cycles of 95°C for 20 seconds, 55°C for 20 seconds, and 72°C for 20 seconds. The sequences of the primers are listed in **Table 1**.

Statistical analysis

No statistical methods were used to predetermine sample sizes; however, animal sample sizes in this study were similar to those reported in previous publications (Dudiki et al., 2020; Wang et al., 2021). Data analyses were conducted using unpaired Student's *t*-tests and Graphpad Prism 8 for Windows (GraphPad Software, Inc., San Diego, CA, USA, www.graphpad.com). Statistical data are presented as means ± SD. A P-value < 0.05 was considered significant.

Table 1 | **Primer sequences and accession number in GenBank database for quantitative reverse transcription-polymerase chain reaction**

Gene	Accession number	Primer sequence (5'–3')
Arg1	NM_007482.3*	F: TCC AAG CCA AAG TCC TTA GAG
		R: AGG AGC TGT CAT TAG GGA CAT C
Cd206	NM_008625.2	F: TCT TTG CCT TTC CCA GTC TCC
		R: TGA CAC CCA GCG GAA TTT C
Nos2	NM_001313922.1	F: CAA GCA CCT TGG AAG AGG AG
		R: AAG GCC AAA CAC AGC ATA CC
Cd86	NM_019388.3	F: GTG TGT GTT CTG GAA ACG GAG
		R: AAC TTA GAG GCT GTG TTG CTG GG
Il4ra	NM_001008700.4	F: ACG TGG TAC AAC CAC TTC CA
		R: GAA CAG GCA AAA CAA CGG GA
β-Actin	NM_007393.5	F: TAT AAA ACC CGG CGG CGC A
		R: TCA TCC ATG GCG AAC TGG TG

*Represents the nucleotide sequence RefSeq accession numbers of the target mRNA on NCBI database. F: Forward; IL: interleukin; R: reverse. Nos2=iNOS.

Results

Progressive RGC loss was observed after transient high IOP-induced RIR injury

RGC loss occurred evenly throughout the retina and became gradually more severe over time (**Figure 1C**). RBPMS$^-$ regions increased progressively over the 28-day period after RIR injury (**Figure 1D**). The quantification of RBPMS$^+$ cells confirmed that RGCs were lost continuously during the 28-day period after RIR injury. Among the adjacent time points, the largest drop in RGC numbers occurred between days 1 and 3. On days 7 and 28, the numbers of RGCs were approximately 50% and 25% of that observed on day 0, respectively (**Figure 1E**).

M2 microglia levels were maximal in the early phase after RIR injury and decreased over time

To investigate the cause of RGC loss, we evaluated changes in microglial polarization after RIR injury. At day 0, the retinal microglia had highly ramified, small cell bodies, which represented resting microglial morphology. After RIR injury, the microglia were activated (**Additional Figure 2A**) and became thicker and less ramified (**Figure 5A**). Panoramas of retinal flat mounts revealed that retinal regions close to the optic nerve had a higher density of RBPMS-poditive cells on day 7; however, the densities of RBPMS-poditive cells were lower in this region than in the peripheral retina on day 14 (**Figure 5B**). The percentage of CD206$^+$ areas peaked on day 7 and eventually decreased to the baseline level on day 28 after RIR injury (**Figure 5C**). The peak time of Cd206 mRNA expression occurred on day 3 (**Figure 5D**). ARG1 protein levels were substantially increased on days 1 and 3 and decreased gradually by day 28 after RIR (**Figure 6B**). Similarly, *Arg1* mRNA expression was maximal on day 3, whereas the expression of the M1-related genes *Cd86* and *iNOS* (Nos2) peaked on day 7 (**Additional Figure 2B**).

A lack of IL-4 in the retina led to decreases in M2 microglia at later time points after RIR

Interestingly, IL-4 could not be detected at any time point (**Figure 6B**). In contrast, *Il4ra* mRNA expression was observed in retinal tissue of mice on day 0, markedly increased on day 3, decreased on day 7, and slightly recovered on day 14; however, expression was reduced to baseline level by day 28 after RIR (**Figure 6A**). IL-4Rα protein in the retinas was substantially increased on day 3 and gradually decreased to the baseline levels by day 28 (**Figure 6B**). The increase in IL-4Rα during the early phase after RIR injury and reduction over time were similar to the changes observed for the M2 microglial markers (**Figure 5D**).

IL-4 administration prolonged the duration of M2 microglia polarization and ameliorated RGC loss in the late stage after RIR injury

IL-4 treatment led to a 6–7-fold increase in both *Arg1* and *Cd206* mRNA and increased *Il4ra* mRNA expression by approximately 1.8-fold compared with vehicle (**Figure 7C**). Double immunostaining for IBA1 and ARG1 demonstrated that the activated microglial population considerably shifted toward the M2 phenotype after IL-4 administration (**Figure 7A**). The percentage of ARG1$^+$ areas in the IL-4 group was > 2 times that in the vehicle group (**Figure 7B**). Furthermore, despite the difference in RGC numbers between the normal (no RIR) and IL-4 groups, exogenous IL-4 treatment improved the survival of RGCs after RIR (**Figure 7D**). The RGC numbers in the IL-4 group were approximately 2 times greater than that in the vehicle group (**Figure 7E**).

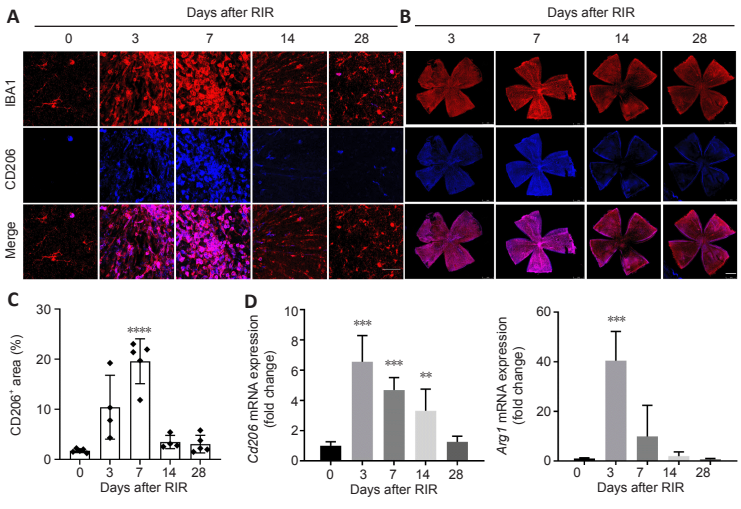

Figure 5 | **M2 microglial levels were maximal in the early phase after RIR injury, decreased over time, and ultimately reached baseline levels.**
Immunofluorescence of IBA1 (red) and CD206 (blue, Alexa Fluor 488) in retinal tissue from mice at 0, 3, 7 14, and 28 days after RIR injury is shown in panels A and B. (A) Representative images for cell counting (scale bar: 50 μm). There were two types of microglial morphology observed in these images: (1) small, highly ramified cell body, which represented resting microglial morphology at day 0 and (2) stockier and less ramified morphology that appeared on activated microglia after RIR. (B) Images of whole retinas (scale bar: 1 mm) indicated that retinal regions close to the optic nerve had a higher density of IBA1$^+$ cells on day 7; however, a lower density of IBA$^+$ cells near the optic nerve was observed on day 14 compared with that in the peripheral retina. All fluorescent images in this study were captured using laser confocal microscopy. In contrast to conventional fluorescence microscopy, the color of the image captured by the confocal microscope is a pseudo-color selected by users rather than the true dye color. We chose blue as the color for CD206 staining out of personal preference. (C) The percent change in CD206$^+$ areas within the retinas over time post-RIR. The CD206$^+$ area peaked on day 7 but eventually decreased to the level of day 0 by day 28 after RIR injury (n = 4–5 mice per group). (D) Bar graph showing the fold change of M2-related genes in retinas for each group compared with that for the day 0 group. *Cd206* and *Arg1* mRNA peaked at day 3 and dropped to the baseline level on day 28 post-RIR (n = 3–4 mice per group). Data are presented as means ± SD. $^{**}P < 0.01$, $^{***}P < 0.001$, $^{****}P < 0.0001$, *vs.* day 0 (unpaired Student's *t*-tests). Three independent replicates were measured for each experiment. IBA1: ionized calcium binding adaptor molecule 1; RIR: retinal ischemia reperfusion.

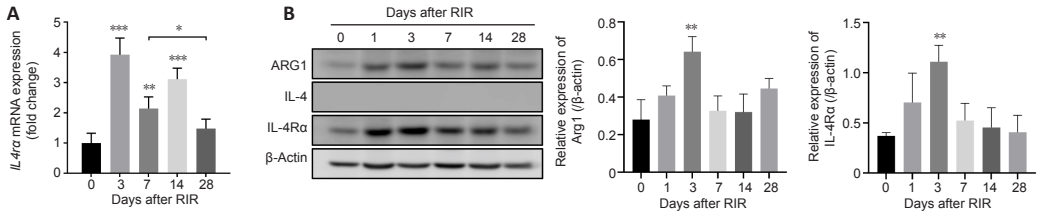

Figure 6 | **Changes in Arg1, IL-4 and IL-4Rα expression after RIR injury.**
(A) Fold change of *Il4ra* mRNA expression in the retinas of mice on days 0, 3, 7, 14, and 28 after RIR injury (quantitative reverse transcription-polymerase chain reaction). The expression of *Il4ra* mRNA was significantly increased on day 3, declined on day 7, and increased again on day 14 after which expression dropped to baseline levels on day 28 after RIR (n = 4 mice per group). (B) Western blot analysis of ARG1, IL-4, and IL-4Rα expression in retinal lysates from mice at 0, 1, 3, 7, 14, and 28 days after RIR. β-Actin was used as a loading control. The grey values were quantified in the histograms (right). n = 3 mice per group. The ARG1 and IL-4Rα protein levels increased on days 1 and 3 and gradually decreased by day 28. IL-4 was not detected in the retina at any time point after RIR (data not shown). $^*P < 0.05$, $^{**}P < 0.01$, $^{***}P < 0.001$, *vs.* day 0 (unpaired Student's *t*-tests). Three independent replicates were measured in each experiment. IL: Interleukin; IL-4Rα: IL-4 receptor α; RIR: retinal ischemia-reperfusion.

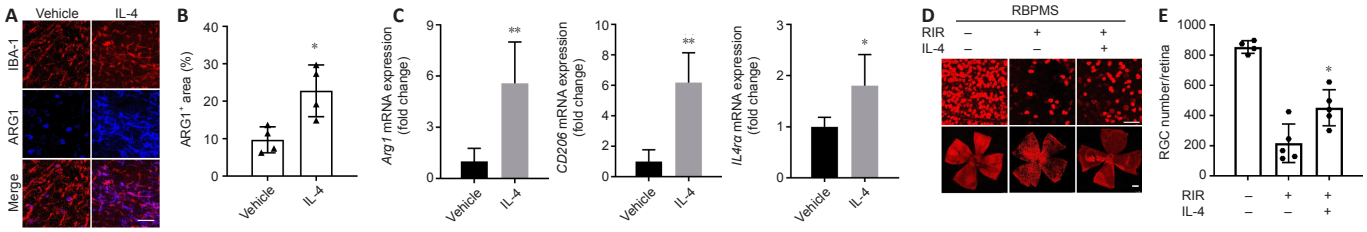

Figure 7 | **Administration of IL-4 prolonged the duration of M2 microglia polarization and improved RGC survival.**
(A) Representative images of retinal flat mounts stained for IBA1 (red) and ARG1 (blue) after treatment with IL-4 or vehicle. These photos suggested that the densities of ARG1$^+$ cells were elevated markedly in RIR mice after IL-4 administration. Scale bar: 50 μm. All fluorescent images in this study were captured by laser confocal microscopy. In contrast to conventional fluorescence microscopy, the colors of the images were pseudo-colors selected by the user rather than the true dye color. We chose blue as the color of ARG1 out of personal preference. (B) Quantification of the percentage of ARG1$^+$ areas in injured retinas treated with IL-4 or vehicle. Retinas from the IL-4 group displayed a greater than 2-fold increase in the ARG1$^+$ area (%) compared with those in the vehicle group (n = 4 mice per group). (C) The mRNA expression of *Il4rα* and M2-related genes in retinas from the vehicle and IL-4 treatment groups. IL-4 treatment led to a 6–7-fold increase in both *Arg1* and *Cd206* mRNA and approximately 1.8-fold increase in *Il4rα* mRNA compared with vehicle (n = 3–5 per group). (D) Representative images of RBPMS expression (red) in retinas from mice 7 days after the last intravitreal dose of IL-4. The upper (scale bar: 50 μm) and lower (scale bar: 1 mm) images were used for cell counting and overall evaluation of RBPMS expression within the whole retina, respectively. The density of RBPMS$^+$ cells in the IL-4 group was higher than that in the vehicle group but less than that in the normal group (RIR and IL-4 negative). (E) Quantification of RGC numbers in retinas from normal, vehicle, and IL-4 groups. The RGC numbers in the IL-4 group were approximately twice greater than that in the vehicle group (n = 4–5 mice per group). Data are presented as means ± SD. *P < 0.05, **P < 0.01, *vs.* vehicle (unpaired Student's t-tests). Three independent replicates were measured for each experiment. IBA1: Ionized calcium binding adaptor molecule 1; IL: interleukin; RBPMS: RNA binding protein, mRNA processing factor; RGC: retinal ganglion cell; RIR: retinal ischemia reperfusion

Discussion

Acute angle-closure glaucoma is a subtype of glaucoma characterized by acute retinal ischemic injury and the loss of RGCs secondary to the elevation of IOP. However, patients with medically controlled IOP may still have progressive visual field loss, suggesting that IOP-independent factors may be involved in RGC loss during the pathogenesis of acute angle-closure glaucoma. Consistent with the results of a previous study (Kim et al., 2013; Nashine et al., 2014), we observed that RGCs were continuously lost after the trigger of high IOP was removed, indicating that a high IOP may be merely an initiator of a multifactorial process leading to RGC apoptosis. Thus, IOP-independent factors may be involved in progressive RGC loss following RIR injury. Retinal glial activation, especially microglial activation, has been implicated in the pathogenesis of glaucoma (Levkovitch-Verbin et al., 2014). Currently, it is commonly believed that, similar to macrophages, microglia can be polarized toward the M0, M1, and M2 phenotypes (Liu et al., 2014; Tanaka et al., 2015). Damage to the CNS induces the polarization of resting microglia toward the proinflammatory M1 phenotype (Kroner et al., 2014). Thus, M1 microglia may be an important target for alleviating neurotoxicity in glaucoma. Consistently, we noted that the mRNA expression of M1-related genes presented an upward trend during the first 7 days after RIR injury, while the opposite trend was observed for M2 microglia.

Microglial polarization toward the M2 phenotype is an adaptive response that promotes tissue repair and regeneration after CNS injury (Prinz and Priller, 2014). As shown in the present study, although M2 microglial polarization was observed, this response was short-lived and began to decrease on day 7 after RIR injury and reached baseline levels on day 28. The persistently low level of M2 microglia in the late phase was likely the primary reason for RGC loss; however, what was the cause of the sharp decline in M2 microglia? To answer this question, we focused on IL-4, which is a predominant cytokine responsible for M2 polarization (Han et al., 2015; Tanaka et al., 2015). Interestingly, we were unable to detect IL-4 mRNA or protein in the mouse retinas, which is consistent with the results from previous studies of other neurodegenerative diseases (Francos-Quijorna et al., 2016; Okutani et al., 2018). However, despite the low level of IL-4Rα detected in the late phase, its expression was markedly upregulated during the early stage after RIR, indicating that retinal microglia can respond to IL-4 soon after activation.

IL-4Rα may function as a molecular switch to promote an M2 phenotype in retinal microglia. Local IL-4 supplementation is possibly the most effective way to 'turn on' this molecular switch. Additionally, IL-4 may also enhance IL-4 receptor expression in microglia via a positive feedback loop by increasing the expression of trophic factors and promoting PPARγ-dependent phagocytosis of apoptotic neurons (Zhao et al., 2015). Our results indicated that, although IL-4 was not produced in the retina, the IL-4 receptor was expressed, which endowed the retina with the capacity to respond to IL-4. The lack of IL-4 may have been responsible for the observed decrease in M2 microglia in the later experimental period because IL-4 administration after RIR injury promoted M2 polarization. Perhaps because of the short half-life of IL-4 in the retina, the local concentration of IL-4 remained insufficient to continuously promote microglial polarization to the M2 phenotype after a single IL-4 injection. As a result, drug administration was performed at three time points, which led to a significantly higher number of M2 microglia at 11 days after RIR. Furthermore, the loss of RGCs was alleviated in the microenvironment with a sustained M2 microglial population, although a difference in RGC numbers remained between the IL-4 supplement group and the no-RIR group. IL-4-mediated M2 microglial polarization after activation and alleviation of neuronal loss in the retina are in line with the results of previous CNS studies (Francos-Quijorna et al., 2016; Kronenberg et al., 2018; Okutani et al., 2018; Song et al., 2019; Zheng et al., 2019; Kobashi et al., 2020). These data verified that endogenous IL-4 in the retina was insufficient to steadily drive microglial polarization toward the M2 phenotype and resulted in RGC death. Exogenous IL-4 administration alleviated RGC loss by prolonging the expression of IL-4Rα and promoting the polarization of M2 microglia.

There were some limitations in this study. There was only one time point used to evaluate the microglia polarization and RGC survival after administrating with IL-4 or vehicle, which lacks a comparison data of days 3, 7, 14, and 28 after RIR. Besides, we assessed the long-term changes in M2 microglial polarization following RIR injury. However, we did not determine the long-term changes in M1 microglia. Although these limitations did not change the results that demonstrated IL-4 promoted M2 microglia polarization and improved RGC survival after RIR, the longer efficiency of IL-4 treatment and the possibility of further reducing RGC damage by lowering M1 microglia polarization should be examined in future studies.

In summary, our data revealed that endogenous IL-4 in the mouse retina is insufficient to maintain microglial polarization toward the M2 phenotype and, subsequently, results in RGC death after RIR. As a result of IL-4Rα expression on retinal microglia, after three intravitreal IL-4 injections, abundant M2 microglial polarization and alleviation of RGC loss were observed during the late experimental phase after RIR, which provides fresh ideas for the treatment of glaucoma.

Author contributions: *WYG and LX conceived of the presented idea and helped supervise the project. DC and CP carried out the experiment with support from XMD, CJZ, YW and LX and contributed to the final version of the manuscript. All authors approved the final version of the manuscript.*
Conflicts of interest: *We declare that we do not have any commercial or associative interest that represents a conflict of interest in connection with the work submitted.*
Availability of data and materials: *All data generated or analyzed during this study are included in this published article and its supplementary information files.*

Additional files:
Additional Figure 1: *Retinal ischemia/reperfusion injury in mice.*
Additional Figure 2: *Expression of IBA1 and M1-related genes in the retina at 0, 3, 7, 14, and 28 days after RIR.*

References

Agarwal R, Agarwal P (2017) Rodent models of glaucoma and their applicability for drug discovery. Expert Opin Drug Discov 12:261-270.

Boche D, Perry VH, Nicoll JA (2013) Review: activation patterns of microglia and their identification in the human brain. Neuropathol Appl Neurobiol 39:3-18.

Burma NE, Bonin RP, Leduc-Pessah H, Baimel C, Cairncross ZF, Mousseau M, Shankara JV, Stemkowski PL, Baimoukhametova D, Bains JS, Antle MC, Zamponi GW, Cahill CM, Borgland SL, De Koninck Y, Trang T (2017) Blocking microglial pannexin-1 channels alleviates morphine withdrawal in rodents. Nat Med 23:355-360.

Chen J, Chen YQ, Shi YJ, Ding SQ, Shen L, Wang R, Wang QY, Zha C, Ding H, Hu JG, Lü HZ (2021) VX-765 reduces neuroinflammation after spinal cord injury in mice. Neural Regen Res 16:1836-1847.

Dudiki T, Meller J, Mahajan G, Liu H, Zhevlakova I, Stefl S, Witherow C, Podrez E, Kothapalli CR, Byzova TV (2020) Microglia control vascular architecture via a TGFβ1 dependent paracrine mechanism linked to tissue mechanics. Nat Commun 11:986.

Francos-Quijorna I, Amo-Aparicio J, Martinez-Muriana A, López-Vales R (2016) IL-4 drives microglia and macrophages toward a phenotype conducive for tissue repair and functional recovery after spinal cord injury. Glia 64:2079-2092.

Grassivaro F, Menon R, Acquaviva M, Ottoboni L, Ruffini F, Bergamaschi A, Muzio L, Farina C, Martino G (2020) Convergence between Microglia and Peripheral Macrophages Phenotype during Development and Neuroinflammation. J Neurosci 40:784-795.

Han A, Yeo H, Park MJ, Kim SH, Choi HJ, Hong CW, Kwon MS (2015) IL-4/10 prevents stress vulnerability following imipramine discontinuation. J Neuroinflammation 12:197.

Hartsock MJ, Cho H, Wu L, Chen WJ, Gong J, Duh EJ (2016) A mouse model of retinal ischemia-reperfusion injury through elevation of intraocular pressure. J Vis Exp:54065.

Hu X, Li P, Guo Y, Wang H, Leak RK, Chen S, Gao Y, Chen J (2012) Microglia/macrophage polarization dynamics reveal novel mechanism of injury expansion after focal cerebral ischemia. Stroke 43:3063-3070.

Kalkman HO, Feuerbach D (2016) Antidepressant therapies inhibit inflammation and microglial M1-polarization. Pharmacol Ther 163:82-93.

Kim BJ, Braun TA, Wordinger RJ, Clark AF (2013) Progressive morphological changes and impaired retinal function associated with temporal regulation of gene expression after retinal ischemia/reperfusion injury in mice. Mol Neurodegener 8:21.

Kobashi S, Terashima T, Katagi M, Nakae Y, Okano J, Suzuki Y, Urushitani M, Kojima H (2020) Transplantation of M2-deviated microglia promotes recovery of motor function after spinal cord injury in mice. Mol Ther 28:254-265.

Kronenberg G, Uhlemann R, Richter N, Klempin F, Wegner S, Staerck L, Wolf S, Uckert W, Kettenmann H, Endres M, Gertz K (2018) Distinguishing features of microglia- and monocyte-derived macrophages after stroke. Acta Neuropathol 135:551-568.

Kroner A, Greenhalgh AD, Zarruk JG, Passos Dos Santos R, Gaestel M, David S (2014) TNF and increased intracellular iron alter macrophage polarization to a detrimental M1 phenotype in the injured spinal cord. Neuron 83:1098-1116.

Lan X, Han X, Li Q, Li Q, Gao Y, Cheng T, Wan J, Zhu W, Wang J (2017) Pinocembrin protects hemorrhagic brain primarily by inhibiting toll-like receptor 4 and reducing M1 phenotype microglia. Brain Behav Immun 61:326-339.

LaPorte SL, Juo ZS, Vaclavikova J, Colf LA, Qi X, Heller NM, Keegan AD, Garcia KC (2008) Molecular and structural basis of cytokine receptor pleiotropy in the interleukin-4/13 system. Cell 132:259-272.

Levkovitch-Verbin H, Waserzoog Y, Vander S, Makarovsky D, Piven I (2014) Minocycline upregulates pro-survival genes and downregulates pro-apoptotic genes in experimental glaucoma. Graefes Arch Clin Exp Ophthalmol 252:761-772.

Liu YC, Zou XB, Chai YF, Yao YM (2014) Macrophage polarization in inflammatory diseases. Int J Biol Sci 10:520-529.

Mantovani A, Biswas SK, Galdiero MR, Sica A, Locati M (2013) Macrophage plasticity and polarization in tissue repair and remodelling. J Pathol 229:176-185.

Mathew B, Ravindran S, Liu X, Torres L, Chennakesavalu M, Huang CC, Feng L, Zelka R, Lopez J, Sharma M, Roth S (2019) Mesenchymal stem cell-derived extracellular vesicles and retinal ischemia-reperfusion. Biomaterials 197:146-160.

Miron VE, Boyd A, Zhao JW, Yuen TJ, Ruckh JM, Shadrach JL, van Wijngaarden P, Wagers AJ, Williams A, Franklin RJM, Ffrench-Constant C (2013) M2 microglia and macrophages drive oligodendrocyte differentiation during CNS remyelination. Nat Neurosci 16:1211-1218.

Murray PJ, Allen JE, Biswas SK, Fisher EA, Gilroy DW, Goerdt S, Gordon S, Hamilton JA, Ivashkiv LB, Lawrence T, Locati M, Mantovani A, Martinez FO, Mege JL, Mosser DM, Natoli G, Saeij JP, Schultze JL, Shirey KA, Sica A, et al. (2014) Macrophage activation and polarization: nomenclature and experimental guidelines. Immunity 41:14-20.

Nashine S, Liu Y, Kim BJ, Clark AF, Pang IH (2014) Role of C/EBP homologous protein in retinal ganglion cell death after ischemia/reperfusion injury. Invest Ophthalmol Vis Sci 56:221-231.

Okutani H, Yamanaka H, Kobayashi K, Okubo M, Noguchi K (2018) Recombinant interleukin-4 alleviates mechanical allodynia via injury-induced interleukin-4 receptor alpha in spinal microglia in a rat model of neuropathic pain. Glia 66:1775-1787.

Olah M, Amor S, Brouwer N, Vinet J, Eggen B, Biber K, Boddeke HW (2012) Identification of a microglia phenotype supportive of remyelination. Glia 60:306-321.

Percie du Sert N, Hurst V, Ahluwalia A, Alam S, Avey MT, Baker M, Browne WJ, Clark A, Cuthill IC, Dirnagl U, Emerson M, Garner P, Holgate ST, Howells DW, Karp NA, Lazic SE, Lidster K, MacCallum CJ, Macleod M, Pearl EJ, et al. (2020) The ARRIVE guidelines 2.0: Updated guidelines for reporting animal research. PLoS Biol 18:e3000410.

Prinz M, Priller J (2014) Microglia and brain macrophages in the molecular age: from origin to neuropsychiatric disease. Nat Rev Neurosci 15:300-312.

Quigley HA (2011) Glaucoma. Lancet 377:1367-1377.

Song Y, Li Z, He T, Qu M, Jiang L, Li W, Shi X, Pan J, Zhang L, Wang Y, Zhang Z, Tang Y, Yang GY (2019) M2 microglia-derived exosomes protect the mouse brain from ischemia-reperfusion injury via exosomal miR-124. Theranostics 9:2910-2923.

Streit WJ, Conde JR, Fendrick SE, Flanary BE, Mariani CL (2005) Role of microglia in the central nervous system's immune response. Neurol Res 27:685-691.

Tanaka T, Murakami K, Bando Y, Yoshida S (2015) Interferon regulatory factor 7 participates in the M1-like microglial polarization switch. Glia 63:595-610.

Tham YC, Li X, Wong TY, Quigley HA, Aung T, Cheng CY (2014) Global prevalence of glaucoma and projections of glaucoma burden through 2040: a systematic review and meta-analysis. Ophthalmology 121:2081-2090.

Wang Y, Gao S, Gao S, Li N, Xie B, Shen X (2021) Blocking the interaction between interleukin-17A and endoplasmic reticulum stress in macrophage attenuates retinal neovascularization in oxygen-induced retinopathy. Cell Biosci 11:82.

Williams PA, Marsh-Armstrong N, Howell GR; Lasker/IRRF Initiative on Astrocytes and Glaucomatous Neurodegeneration Participants (2017) Neuroinflammation in glaucoma: a new opportunity. Exp Eye Res 157:20-27.

Xiong X, Xu L, Wei L, White RE, Ouyang YB, Giffard RG (2015) IL-4 is required for sex differences in vulnerability to focal ischemia in mice. Stroke 46:2271-2276.

Zanier ER, Pischiutta F, Riganti L, Marchesi F, Turola E, Fumagalli S, Perego C, Parotto E, Vinci P, Veglianese P, D'Amico G, Verderio C, De Simoni MG (2014) Bone marrow mesenchymal stromal cells drive protective M2 microglia polarization after brain trauma. Neurotherapeutics 11:679-695.

Zhang W, Tian T, Gong SX, Huang WQ, Zhou QY, Wang AP, Tian Y (2021) Microglia-associated neuroinflammation is a potential therapeutic target for ischemic stroke. Neural Regen Res 16:6-11.

Zhao X, Wang H, Sun G, Zhang J, Edwards NJ, Aronowski J (2015) Neuronal interleukin-4 as a modulator of microglial pathways and ischemic brain damage. J Neurosci 35:11281-11291.

Zheng Y, He R, Wang P, Shi Y, Zhao L, Liang J (2019) Exosomes from LPS-stimulated macrophages induce neuroprotection and functional improvement after ischemic stroke by modulating microglial polarization. Biomater Sci 7:2037-2049.

C-Editor: Zhao M; S-Editor: Li CH; L-Editors: Zunono S, Li CH, Song LP; T-Editor: Jia Y

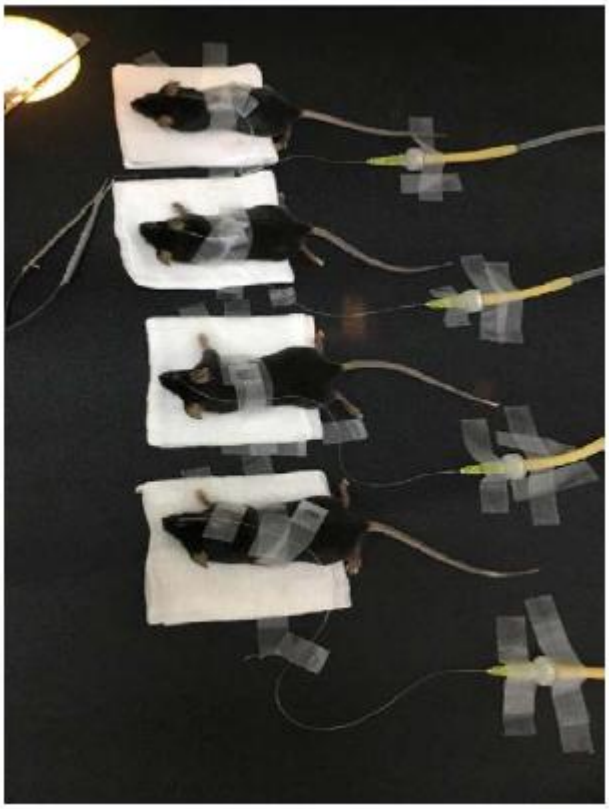

Additional Figure 1 Retinal ischemia-reperfusion injury in mice.

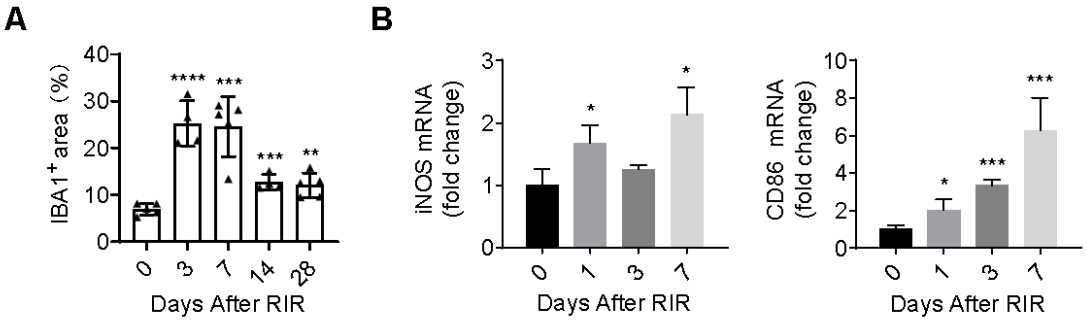

Additional Figure 2 Expression of IBA1 and M1-related genes in the retina at 0, 3, 7, 14, and 28 days after RIR.

(A) Quantification of IBA1$^+$ area % (immunofluorescent staining). n = 3–5 mice/group (unpaired Student's t-test). (B) Changes in the expression of M1-related genes determined by quantitative reverse transcription-polymerase chain reaction. The data are presented as means ± SD. **P* < 0.05, ***P* < 0.01, ****P* < 0.001, vs. day 0; n = 3–4 mice/group (unpaired Student's t-test). Three independent replicates were measured in each experiment. IBA1: ionized calcium binding adaptor molecule 1; RIR: retinal ischemia-reperfusion. iNOS=*Nos2*.